


## Article

# The Effect of Chelate Compounds on the Hydration Process of MgO–Al<sub>2</sub>O<sub>3</sub> Phase System under Hydrothermal Conditions

Ryszard Prorok <sup>1,\*</sup>, Jakub Ramult <sup>1</sup>, Wiesława Nocun-Wczelik <sup>2</sup> and Dominika Madej <sup>1</sup> 
<sup>1</sup> Department of Ceramics and Refractories, Faculty of Materials Science and Ceramics, AGH University of Science and Technology, al. A. Mickiewicza 30, 30-059 Krakow, Poland; jramult@agh.edu.pl (J.R.); dmadej@agh.edu.pl (D.M.)

<sup>2</sup> Department of Building Materials Technology, Faculty of Materials Science and Ceramics, AGH University of Science and Technology, al. A. Mickiewicza 30, 30-059 Krakow, Poland; wiesia@agh.edu.pl

\* Correspondence: rprorok@agh.edu.pl

**Featured Application:** In the field of the design and production of refractory materials, this work will allow a better understanding of the changes that take place during the first stage of the heat treatment of the castables, related to the decomposition of the hydraulic bond in the castables matrix.

**Abstract:** In refractory castables during heat treatment, there is a dynamic change from a hydraulic bond to a ceramic bond. During heating, the emission of water takes place; this changes the conditions inside the material to something similar to the hydrothermal ones. This influences the processes that occur during the heating of the castables, and in consequence, the properties of the final material. The aim of the work was to evaluate the influence of the chelate compounds like citric and tartaric acids, often used in castables as dispersing agents, on the properties of the MgO–Al<sub>2</sub>O<sub>3</sub> phase system during hydrothermal treatment. The performed tests included an XRD analysis, a thermal analysis (TG–DSC–EGA), infrared spectroscopy (FTIR), and an SEM–EDS analysis. Based on the obtained results, it was found that even small amounts of chelate compounds have a strong impact on the processes under hydrothermal conditions which results in changes in the phase composition of the materials.

**Keywords:** castables; hydration; hydraulic binders; heat treatment; refractory



**Citation:** Prorok, R.; Ramult, J.; Nocun-Wczelik, W.; Madej, D. The Effect of Chelate Compounds on the Hydration Process of MgO–Al<sub>2</sub>O<sub>3</sub> Phase System under Hydrothermal Conditions. *Appl. Sci.* **2021**, *11*, 2834. <https://doi.org/10.3390/app11062834>

Academic Editor: Theodore Matikas

Received: 4 February 2021

Accepted: 3 March 2021

Published: 22 March 2021

**Publisher's Note:** MDPI stays neutral with regard to jurisdictional claims in published maps and institutional affiliations.



**Copyright:** © 2021 by the authors. Licensee MDPI, Basel, Switzerland. This article is an open access article distributed under the terms and conditions of the Creative Commons Attribution (CC BY) license (<https://creativecommons.org/licenses/by/4.0/>).

## 1. Introduction

Castables are a wide group of materials, one of the main features of which is the heat treatment process during preparation. The reactions of synthesis and sintering of the materials are activated by high temperatures. Alumina–magnesia spinel is a compound with a wide application in ceramic materials, as well as an important component of alumina spinel refractory castables. The solid-state synthesis of the spinel from oxide powders is the most popular route to obtaining it for an industrial purpose. During this process, the reaction proceeds according to the Wagner model. According to it, the spinel synthesis reaction is a diffusion process (counter-directed diffusion of Mg and Al ions while oxide ions remain on the initial sites), which is activated by the temperature. However, due to a low diffusion coefficient and also the formation of a diffusion-impeding product layer, the process of spinel synthesis is very costly [1]. Moreover, the mixing of the spinel component in the refractories generates problems with obtaining a fully homogeneous distribution in the material. For those reasons, the so-called insitu synthesis of spinel is used. In this kind of process, the spinel is generated from the substrates directly in the refractory castables, during high-temperature heat treatment. However, in this method, the presence of water modifies the course of the synthesis reaction. The starting substrates are not only oxides but also hydroxides of magnesium, and aluminum, and the conditions in the material during the increase in temperature become similar to the hydrothermal ones. This is the difference

between the classical solid state synthesis of the spinel and the insitu synthesis of this phase in castables. Although spinel solid state synthesis from oxides is well characterized [1–8], there is still a lack of knowledge about the insitu synthesis of the spinel in refractory castables, especially at the early stage of such a reaction at the temperature level where water vapor can be present.

In refractory castables, oxide powders are used as substrates in spinel synthesis. In contrast to the solid-state reaction in the castables, the synthesis of the spinel takes place in several intermediate stages. In the first step, during the preparation of the castable, the oxide powders hydrate. During the heat treatment, hydraulic compounds undergo parallel dehydration and also rehydration due to high water vapor pressure, after further temperature increase; all these hydraulic phases convert to oxides which react to form the spinel phase. According to [9], this sequence of the reaction influences the properties of the synthesized spinel. The spinel formed insitu in such a process has a lower formation temperature, lower crystal size, and is better dispersed in the castables. This provides outstanding corrosion resistance and improves the high-temperature properties of the castables [9–11].

According to the  $\text{MgO-Al}_2\text{O}_3\text{-H}_2\text{O}$  phase system, at low temperatures, characteristic for preparing and curing castables, the reaction of magnesium oxide and alumina oxide with water leads to the formation of magnesium hydroxide, aluminum hydroxide, and Mg/Al layered double hydroxides (LDH) and in the case of the presence of  $\text{CO}_2$  in the system also of hydrotalcite. The hydration reaction of  $\text{Al}_2\text{O}_3$  in ambient temperature in the refractory castables is usually connected with transition alumina. During the rapid hydration of transition alumina at elevated pH, the main crystalline product is bayerite rather than gibbsite. In these conditions,  $\alpha\text{-Al}_2\text{O}_3$  is inert, but this could change depending on the conditions like pH, temperature and water vapor pressure. Magnesium oxide is transformed to brucite as one stable polymorph of magnesium hydroxide and both  $\text{MgO}$  and  $\text{Al}_2\text{O}_3$  can create DHL or hydrotalcite-like compounds [12,13].

Due to the presence of  $\text{MgO}$  in the castables, aids are also used that influence the hydration process, like amorphous silica, chelate compounds, etc. These compounds strongly modify the hydration process. Chelates like citric and tartaric acids modified the hydration process in this system. In a high pH environment, which is characteristic for systems with  $\text{MgO}$ , citric as well as tartaric acids dissociated. The dissociation of these compounds depends on the pH of the environment and for pastes from  $\text{MgO-Al}_2\text{O}_3\text{-H}_2\text{O}$  system, it exceeds 10. In such conditions, both the citric and tartaric acids are present in the fully dissociated forms,  $\text{C}_6\text{H}_5\text{O}_7^{3-}$  and  $\text{C}_4\text{H}_4\text{O}_6^{2-}$ . This provides them with the ability to adsorb the positive charges on the surface of the grains and create a complex with metal ions in solution. The neutralization of the net surface charge and coordination of the Mg/Al ions prevent magnesium oxide grains from dissolution and precipitation of the hydroxides and decrease the rate of hydration process in a water solution. However, during the heat treatment at an elevated temperature, reactions in this system are accelerated by the high-water vapor pressure that prevails in castables [13–17].

Reactions that occur at the early stage of the heat treatment of the castables have a key role in shaping the properties of these materials. This, in consequence, decides about the course of many high-temperature reactions like the spinel synthesis. The aim of this study was to evaluate the effect of the two most popular chelating agents used in castables, citric and tartaric acids, on the phases coexisting in the  $\text{MgO-Al}_2\text{O}_3\text{-H}_2\text{O}$  system, under hydrothermal conditions. Hydrothermal conditions are designed to simulate conditions that are prevailing in large volume castables precast units during the heat treatment.

## 2. Materials and Methods

High-purity, reagent grade magnesium oxide powder ( $\text{MgO} \geq 98\%$  from Acros Organics, Geel, Belgium), commercial reactive alumina powder ( $d_{50} \leq 0.6 \mu\text{m}$ ,  $\text{Al}_2\text{O}_3 \cong 99.8\%$ , RG 4000 from Alantis, Leetsdale, PA, USA), citric acid ( $\text{C}_6\text{H}_8\text{O}_7 \cdot \text{H}_2\text{O} \geq 99.5\%$  from POCH, Gliwice, Poland), and tartaric acid ( $\text{C}_4\text{H}_4\text{O}_6 \geq 99\%$  from POCH) were used as raw

materials. Pictures of the raw materials are shown in Figure 1. The magnesium oxide and alumina powder were mixed at a 1:1 molar ratio, and their samples' compositions are presented in Table 1.

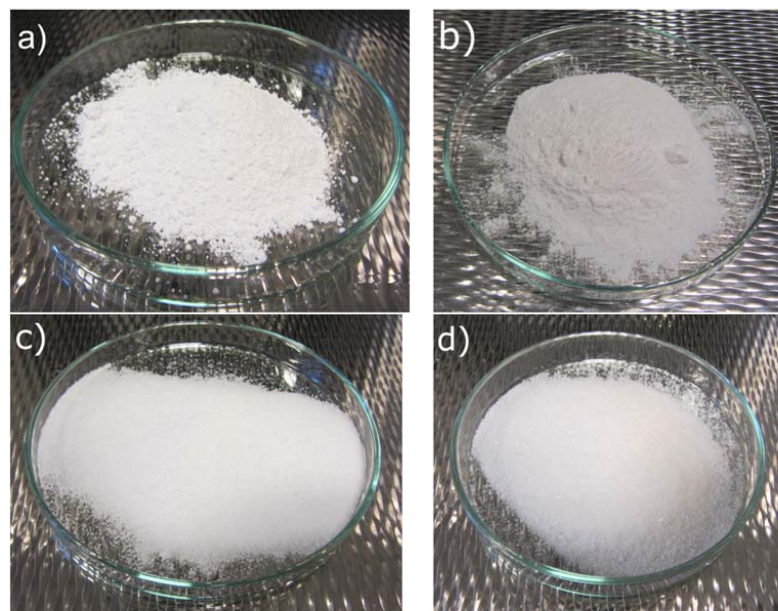


**Figure 1.** Raw materials used in the experiment: (a) alumina powder RG 4000; (b) magnesium oxide powder; (c) citric acid; and (d) tartaric acid.

**Table 1.** Composition of the studied samples.

Sample	A <sub>2</sub> O <sub>3</sub> (% mas.)	MgO (% mas.)	Citric Acid (% mas.)	Tartaric Acid (% mas.)	Sum (% mas.)
1	71.67	28.33	-	-	100
2	70.95	28.05	1	-	100
3	70.95	28.05	-	1	100

Powders of the raw materials were homogenized by mechanical mixing in a planetary mill using rubber mixing elements, pressed into pellets (diameter 20 mm, under the pressure of 20 MPa), and subjected to a hydrothermal synthesis at the temperature of 240 °C, under autogenous water vapor pressure for 8 h.

The samples, obtained after a hydrothermal treatment, have a powder form. The samples were washed several times with cold acetone to remove free water. Samples for the thermal analysis, XRD analysis as well as FTIR analysis were subjected to grinding in a mortar grinder to obtain powder samples under 0.063 mm.

To identify the samples' phase changes corresponding to the used additives, the X-ray diffraction (XRD), Fourier transform infrared spectroscopy (FTIR), and thermal analysis, i.e., thermogravimetry (TG), differential scanning calorimetry (DSC), and evolved gas analysis–mass spectrometry (EGA–MS), were simultaneously used. The chemical composition and the microstructure of the samples were characterized by scanning electron microscopy (SEM) with energy dispersive spectroscopy (EDS).

The thermal analysis was carried out using a Simultaneous Thermo Analyzer (STA) TG–DSC NETZSCH STA 449F5 Jupiter coupled to QMS 403 D Aëolos (Erich NETZSCH GmbH & Co. Holding KG, Selb, Germany). The provided sample mass ~30 mg was heated to 1000 °C in airflow (50 mL/min) at a heating rate of 10 °C/min, in a corundum crucible.

The XRD measurement was carried out using an X'PertProPANalytical X-ray diffractometer, in the range of 5–90 2θ, with Cu Kα radiation, with 0.02° per step and a time of 3 s

per step. Data analysis was made by HighScore Plus software (Panalytical) with the PDF-2 database supported by the ICDD (The International Centre for Diffraction Data, Newtown Square, PA, USA), the full list of reference patterns is provided in Table 2.

**Table 2.** Phase composition of the studied samples.

Sample Designation	Identified Phase	Reference Pattern
1	$\alpha$ -Aluminum oxide $\text{Al}_2\text{O}_3$	01-088-0826
	Boehmite $\text{AlO}(\text{OH})$	01-083-2384
	Aluminum oxide hydrate $11\text{Al}_2\text{O}_3 \cdot 1.79\text{H}_2\text{O}$	01-070-0384
	Double magnesium aluminum hydroxide hydrate $\text{Mg}_6\text{Al}_2(\text{OH})_{18} \cdot 4.5\text{H}_2\text{O}$	00-035-0965
	Brucite $\text{Mg}(\text{OH})_2$	00-044-1482
2	Aluminum oxide $\text{Al}_2\text{O}_3$	01-088-0826
	Boehmite $\text{AlO}(\text{OH})$	01-083-2384
	Aluminum oxide hydrate $11\text{Al}_2\text{O}_3 \cdot 1.79\text{H}_2\text{O}$	01-070-0384
	Double magnesium aluminum hydroxide hydrate $\text{Mg}_6\text{Al}_2(\text{OH})_{18} \cdot 4.5\text{H}_2\text{O}$	00-035-0965
	Brucite $\text{Mg}(\text{OH})_2$	00-044-1482
	Periclase $\text{MgO}$	00-004-0829
3	Aluminum oxide $\text{Al}_2\text{O}_3$	01-088-0826
	Boehmite $\text{AlO}(\text{OH})$	01-083-2384
	Aluminum oxide hydrate $11\text{Al}_2\text{O}_3 \cdot 1.79\text{H}_2\text{O}$	01-070-0384
	Double magnesium aluminum hydroxide hydrate $\text{Mg}_6\text{Al}_2(\text{OH})_{18} \cdot 4.5\text{H}_2\text{O}$	00-035-0965
	Brucite $\text{Mg}(\text{OH})_2$	00-044-1482
	Periclase $\text{MgO}$	00-004-0829

The IR bands were recorded using a Bruker Vertex 70v FTIR spectrometer at a spectral range of  $400\text{--}4000\text{ cm}^{-1}$ . Measurements were carried out on pelletized ca. 0.5 wt.% powder samples in a KBr matrix.

The microstructure images were carried out using a Nova Nano SEM 200 FEI (FeiEurope Company, Eindhoven, Netherlands). Measurements were recorded using a low vacuum detector (LVD) using secondary electrons (SE). Chemical analysis was carried out using an EDS analyzer (EDAX corporate, Mahwah, NJ, USA).

### 3. Results

According to the XRD analysis shown in Figure 2 and summarized in Table 2, the phase composition is very similar for each sample. The XRD spectra indicate the presence of a number of hydrated phases in each sample. Brucite ( $\text{Mg}(\text{OH})_2$ ) is the first of the phases connected with magnesium oxide, the second identified phase is double magnesium and aluminum hydroxide hydrate ( $\text{Mg}_6\text{Al}_2(\text{OH})_{18} \cdot 4.5\text{H}_2\text{O}$ ). In the samples, aluminum oxide hydroxide ( $\text{AlO}(\text{OH})$ ) and a form of hydrated aluminum oxide with a formula close to  $11\text{Al}_2\text{O}_3 \cdot 1.79\text{H}_2\text{O}$  were also observed. The non-hydrated oxides in the studied samples were aluminum oxide ( $\text{Al}_2\text{O}_3$ ), present in each sample, and traces of  $\text{MgO}$  for the sample with the addition of chelates. Based on this result, it can be stated that magnesium oxide, in the experimental conditions, completely reacted with water for sample 1 while some traces of it remained in the sample with the addition of citric and tartaric acids. According to the XRD analysis, there were no traces of aluminum hydroxide in the samples, although, in the experimental conditions, bayerite should have probably appeared [13]. In the place of aluminum hydroxide, boehmite can be identified, and magnesium aluminum hydroxide

hydrate can be observed. However, the amount of the double magnesium alumina hydroxide is rather low in respect to boehmite, it suggests that that if aluminum hydroxide appears during the hydrothermal treatment, it converts into boehmite rather than into double magnesium and aluminum hydroxide. Depending on the author, gibbsite formation takes place in the temperature of at least ca. 130–150 °C (these are the lowest values provided in the literature). When the temperature exceeds these values, direct formation of boehmite starts to be preferable [18–21]. According to [22], gibbsite in the experimental conditions could be decomposed with the creation of boehmite around 230 °C, but bayerite with the temperature of decomposition around 280–300 °C should still be stable. This suggests that when increasing the temperature to the maximum assumed value (240 °C) in the experiment, the hydration process proceeds with gibbsite synthesis as an intermediate stage. It should also be noted that in the temperature range of this experiment, the water vapor pressure does not affect the alumina hydration [18,21].

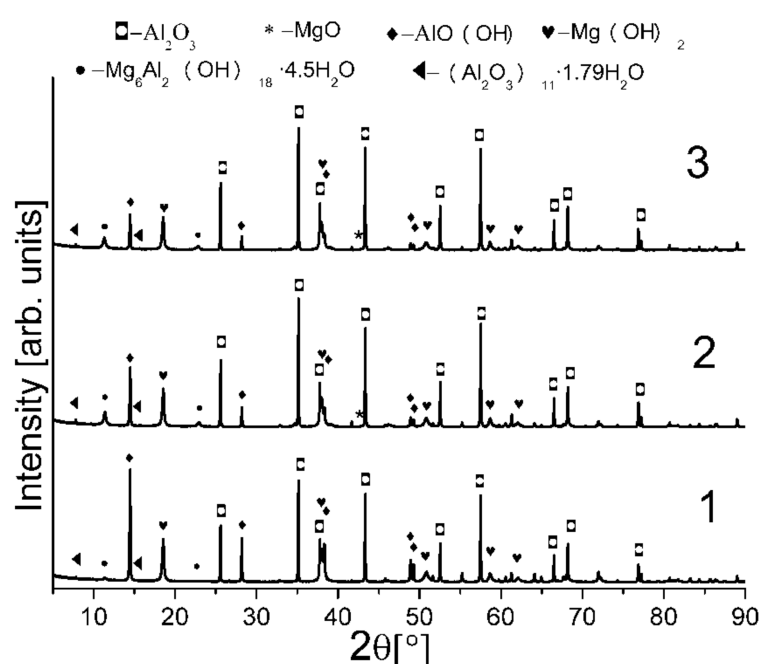


**Figure 2.** X-ray diffraction spectra of studied samples (1—reference sample; 2—sample with citric acid addition; and 3—sample with tartaric addition).

It needs to be emphasized that double magnesium and aluminum hydroxide hydrate easily form hydrotalcite-like compounds in the presence of carbon dioxide. However, there is no evidence of such a reaction on the XRD spectra, although the crystal structures of both phases are very similar [10,23].

Based on the results of the thermal analysis, it can be observed that the course of changes in the case of samples with acids additions is almost the same, while for the reference sample it varies (Figure 3).

For each sample, three main endothermic effects connected with the loss of mass of the samples can be observed. The first of those effects is placed around 186–202 °C and can be connected with the first step of decomposition of double magnesium and aluminum hydroxide and emission of interlayer water. These findings are confirmed on the EGA–MS curve ( $m/z = 18$ ), where the effect from water ions is observed. Moreover, the non-symmetrical character of this effect (longer arm for the lower range of temperatures) can indicate the amorphous character of double magnesium aluminum hydroxide hydrate or/and decomposition in this temperature range an additional phase, probably aluminum oxide hydrate [10,24].



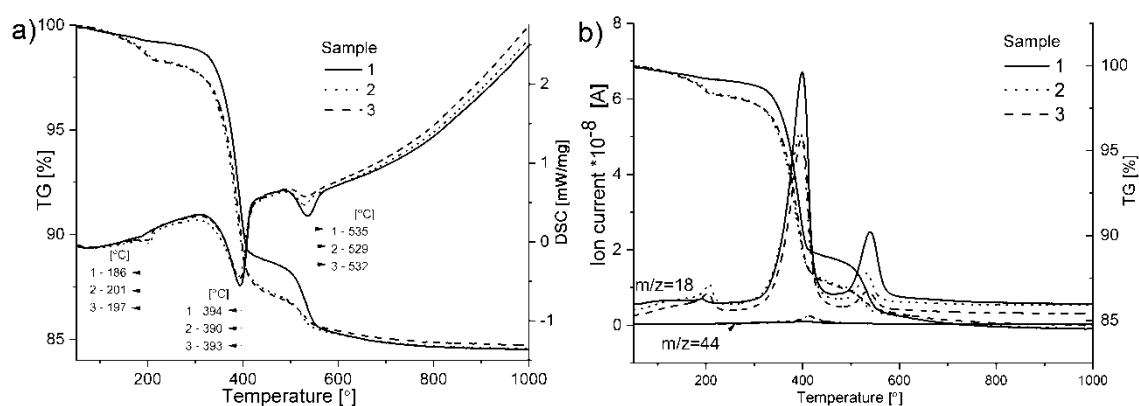


**Figure 3.** Thermal analysis of studied samples, (a) TG-DSC, (b) TG-EGA.

At around 390 °C, another endothermic effect occurs, probably connected with the dihydroxylation of brucite and the second step of the decomposition of double magnesium and aluminum hydroxide hydrate. This effect is connected with the emission of CO<sub>2</sub> with the maximum at ca. 413 °C (Figure 3b, EGA curve for  $m/z = 44$ ); this could be the evidence of the last stage of decomposition of hydrotalcite-like compounds. Despite the results of the XRD analysis, the short range of the temperature of this effect as well as the profile of the TG curve with a sharp loss of mass in this region do not fully support this claim, as some amount of poorly crystalline hydrotalcite-like phase maybe present in the samples [9,10,24,25]. At the temperature around 530 °C, the decomposition of boehmite follows [10].

Each of the above effects is connected with mass loss shown in Figure 4. During the first endothermal effects (up to 250 °C), the loss of mass of the samples was from around 0.81% mass for a sample without any additions, up to 1.82% for sample number 3 with an addition of tartaric acid. In the second effect, the loss of mass of the samples increases, also a sample with tartaric acid addition has the highest loss around 10.93% while the reference sample has only a loss of 10.35%. Taking into consideration that in the samples with an addition of chelates, MgO does not fully hydrate, it shows a strong influence of decomposition of double magnesium and aluminum hydroxide hydrate or/and hydrotalcite on a loss of mass in this range. Conversely, in the last identified effect, sample 1 has the highest loss of mass around 3.73% while the sample with tartaric acid has a loss of around 2.04%. The losses of mass and temperatures of the individual effects suggest that the qualitative phase composition is the same for each sample, and the depth of each effect is proportional to the content of the individual phases. This claim is supported by an XRD analysis. This is why, when taking into consideration the results of the thermal analysis, it can be stated that the addition of acids to the MgO–Al<sub>2</sub>O<sub>3</sub>–H<sub>2</sub>O system changes the phase composition in respect to its quantitative composition.

The summary of the thermal effect with the loss of mass from the thermal analysis is shown in Table 3.

Comparing the loss of mass in each effect, it can be noticed that in the two first effects, the loss is arranged in order from sample number 1, 2 and 3 at the end. In the case of the third effect, the order is the opposite. The relative content of the phases in each studied sample can be investigated by an XRD analysis by the comparison of the characteristic diffractive lines for each sample. Aluminum oxide has its main diffraction line at 35.137° 2θ (ICSD 01-088-0826) and as the main substrate, can indicate the overall content of the reacted aluminum phases. As it is shown in Figure 5a, sample 2 with citric acid additions has the highest intensity of the diffractive line and associated with it the highest amount of Al<sub>2</sub>O<sub>3</sub>, a slightly lower amount is in the sample with tartaric acid and the lowest amount of aluminum oxide in the reference sample. Taking into consideration the spectral lines for other phases, these relationships are also visible. Consequently, for the main diffraction line for boehmite shown in Figure 5b, the intensity changes in opposition to aluminum

oxide. Reference sample 1 has the highest intensity, followed by the sample with citric acid and at the end is the sample with tartaric acid. This confirms the findings of the thermal analysis, where losses of mass in the last endothermic effect associated with the decomposition of boehmite were in the same order. In the case of Mg-containing phases, the results also show a strong relationship between the addition of citric and tartaric acids and the composition of each sample. In the case of brucite (due to the overlapping of its main diffractive line with peaks for others phases, the second most intensive diffractive line was utilized), we can observe (Figure 5c) that the addition of acids decreases its content in the samples but simultaneously increases the amount of double magnesium aluminum hydroxide hydrate in relation to the reference sample (Figure 5d). The relation in the case of brucite would be in agreement with both the observed amount of double magnesium aluminum hydroxide hydrate and the traces of MgO in samples with chelates addition revealed in the XRD analysis.

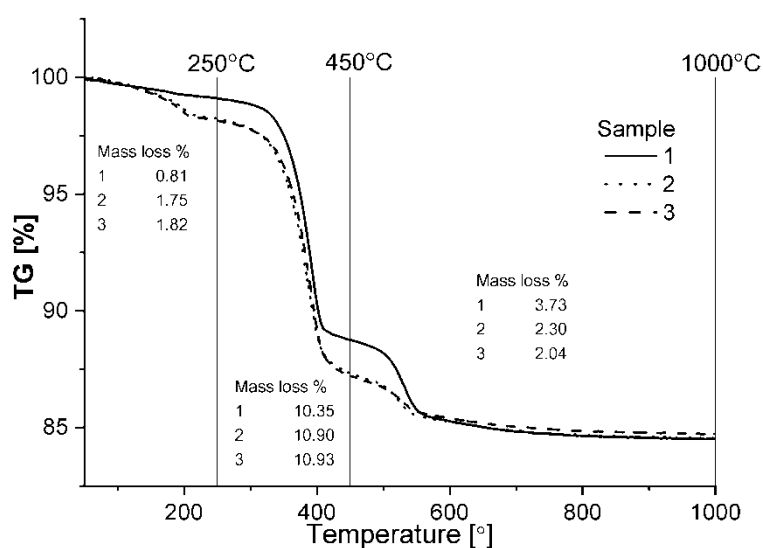


**Figure 4.** Thermogravimetric analysis of the studied samples with a loss of mass in a specific range of temperature.

**Table 3.** Summary of the thermal effect and a loss of mass in a specified range of temperature.

Sample	Character of the Effect	Temperature of Maximum of the Effect * (°C)	Range of Temperatures of the Effect ** (°C)	Mass Loss Connected with the Effect (%)
1	Endothermic	186.1	40–250	0.81
	Endothermic	394.4	250–450	10.35
	Endothermic	535.9	450–1000	3.73
2	Endothermic	201.8	40–250	1.75
	Endothermic	390.1	250–450	10.90
	Endothermic	529.4	450–1000	2.30
3	Endothermic	197.5	40–250	1.82
	Endothermic	393.2	250–450	10.93
	Endothermic	532.6	450–1000	2.04

\* based on a DSC curve. \*\* based on a TG curve.

Taking into consideration the results from the XRD analysis and thermal analysis, the strong influence of acid additions on the hydration process of the studied samples under hydrothermal conditions can be stated.

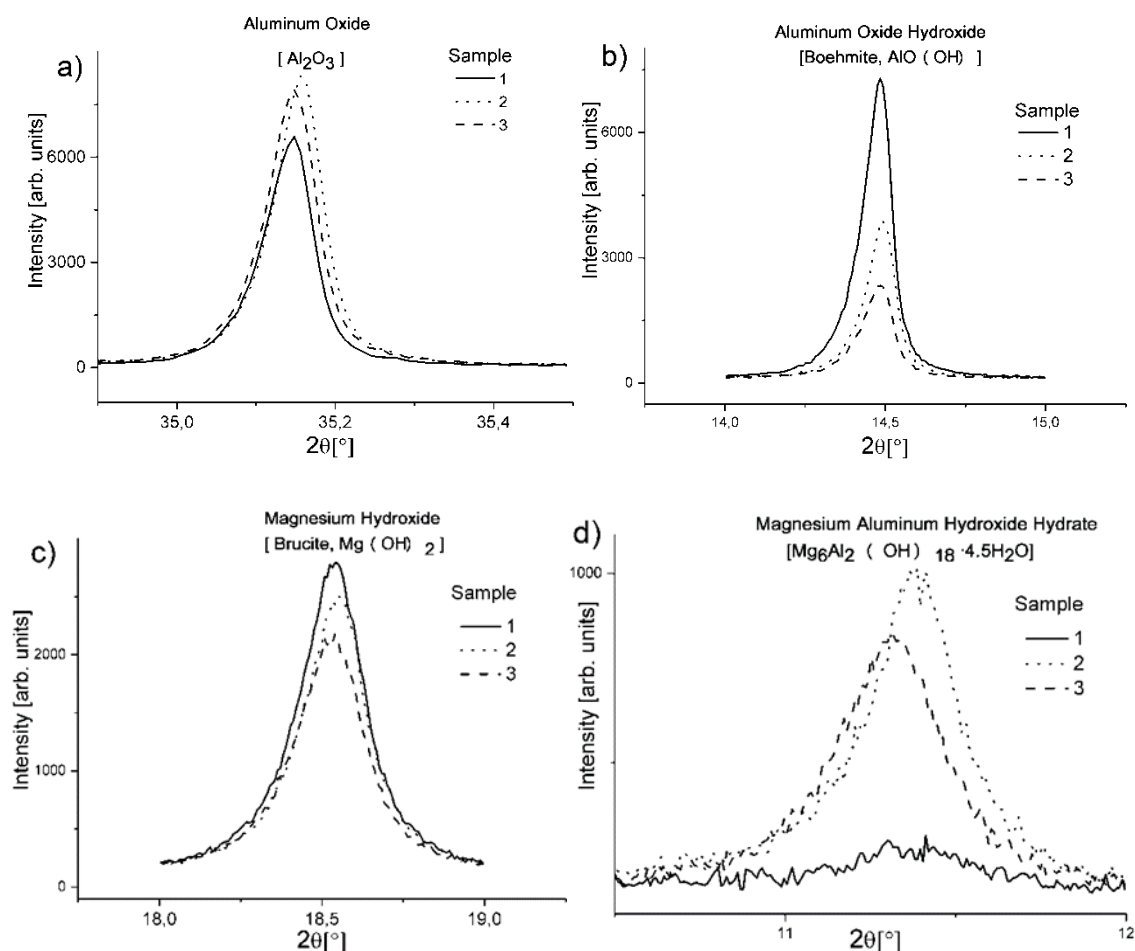


**Figure 5.** Comparison of the characteristic XRD peaks for a specified phase: (a) Al<sub>2</sub>O<sub>3</sub>; (b) AlO(OH); (c) Mg(OH)<sub>2</sub>; and (d) Mg<sub>6</sub>Al<sub>2</sub>(OH)<sub>18</sub>·4.5H<sub>2</sub>O.

The spectra of FTIR spectroscopy shown in Figure 6 reveal several bands characteristic for hydrated phases that can confirm the previous results. The broad bands in the range of 3000–3700 cm<sup>−1</sup> are mainly connected with hydroxyl groups (−OH), bonded with the metal hydroxide layers. Worthy of notice is the sharp envelope of this band, which indicates a high degree of crystallinity of the studied samples in this aspect. First of these bands, around 3695 cm<sup>−1</sup> is present in each sample, which is connected with −OH groups in octahedral brucite layers [9,26]. Around 3200–3250 cm<sup>−1</sup> as well as 3400–3450 cm<sup>−1</sup> are often located bands assigned to non-structural water vibration [27], although in the range of around 3450 cm<sup>−1</sup> according to [9,24] where the stretching vibrations of the −OH groups attached to Mg and Al ions are also located. Band ca. 3086–3088 cm<sup>−1</sup> can be attributed to the −OH bond [28].

Bands connected with bending vibrations of water molecules are located around 1639–1647 cm<sup>−1</sup> [10,29]. While the bands around 1370–1460 cm<sup>−1</sup> can be attributed to stretching vibrations from the carbonate anion [9,10]. These vibrations are often connected with hydrotalcite. Taking into consideration these bands as well as the results of the thermal analysis, it can be stated that in the studied samples, there is some hydrotalcite-like phase. Comparing the relative intensity of this band in the spectra for each sample, it can be noticed that the higher relative intensity of these bands occurs in the samples with the additives. This suggests that in this samples content of hydrotalcite like phase is higher. Worthy of notice is that some authors [15] connect the band ca. 1380 cm<sup>−1</sup> with deformation vibrations of C–O in adhered tartaric acid to the crystals of the ceramic phases.



The band at  $1072\text{ cm}^{-1}$  corresponds to symmetric bending vibrations of the Al–O–H mode in boehmite [28].

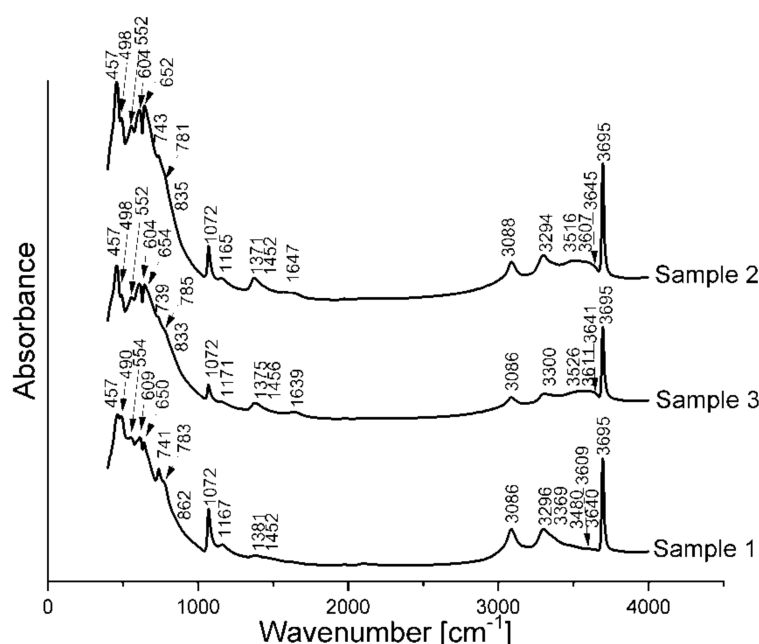


Figure 6. FTIR spectra of studied samples.

Bands ca.  $740$ ,  $780$ ,  $830$ – $860\text{ cm}^{-1}$  are attributed to Al–O vibrations mode in boehmite. Vibrations of M–O and M–OH (where M is a metal ion—Al or Mg) in octahedral metal layer are associated with the region around  $400$ – $650\text{ cm}^{-1}$ . Bands ca.  $552\text{ cm}^{-1}$  are connected with Al–OH and  $600$ – $650\text{ cm}^{-1}$  with Mg–OH translations mode [9,10,28].

The FTIR analysis confirms the results from the thermal analysis and XRD analysis; moreover, it indicates the presence of the hydrotalcite-like phase in the studied samples.

The SEM–EDS analysis shows only slight differences between the samples. The microstructure of the samples shown in Figure 7 consists of two kinds of granularly shaped grains. The smaller ones are loosely connected with each other and create a matrix for larger grains. According to the EDS analysis, their chemical composition is varied, and larger aggregates have a higher amount of aluminum with an admixture of magnesium and various levels of oxide. This suggests boehmite or/and aluminum oxide as the main component(s) of these grains. While smaller aggregates have a higher content of magnesium and a high level of oxide, this indicates that magnesium hydroxide and/or double magnesium and aluminum hydroxide hydrate are the main components of these grains. These findings are in agreement with the result of the previous analysis.

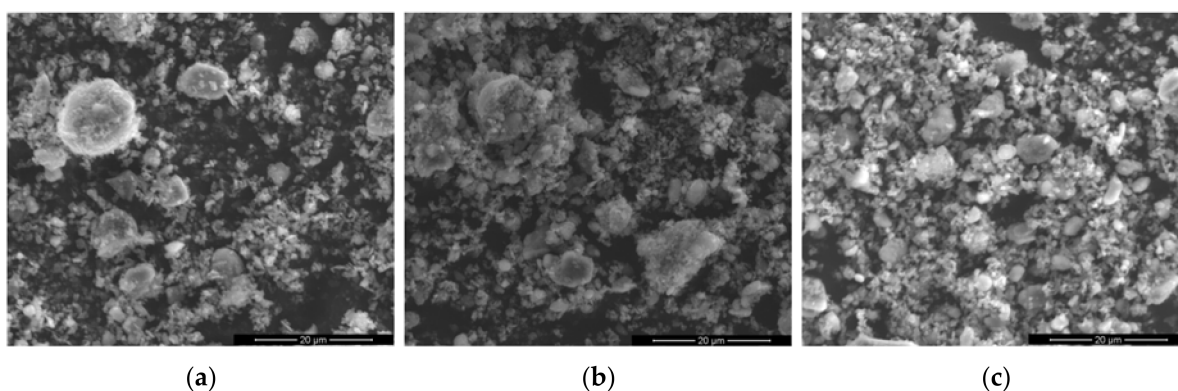


Figure 7. SEM images of the studied samples: (a) sample 1; (b) sample 2; and (c) sample 3.

#### 4. Discussion

This work explains the reactions and the process that occur under hydrothermal conditions in the  $\text{MgO-Al}_2\text{O}_3\text{-H}_2\text{O}$  system with chelates addition. The aim of the utilization of the hydrothermal conditions was to simulate the conditions that prevail during the first stage of the high temperature heat treatment of the refractory castables up to ca. 500–600 °C. In this range of temperature, most of the hydraulic phases undergo a decomposition with the creation of ceramic phases. Newly created ceramic phases are often altered in comparison with the original raw materials used in the castables' composition. They have smaller crystallites and are better dispersed and connected with each other, thanks to the synthesis of many new phases like spinel, etc., which takes place at a lower temperature. Chelates like citric and tartaric acid are often used in castables as dispersing agents: from the presented result, it was found that chelates affect the hydration behavior of  $\text{MgO}$  and  $\text{Al}_2\text{O}_3$ .

According to the XRD analysis results (Figure 2), it can be stated that among other hydraulic phases, samples are also consisting of double magnesium aluminum hydroxide hydrate. However, the thermal analysis shows (Figure 3b) the emission of carbon dioxide in the temperature range of 280–550 °C is probably connected with the second endothermic effect at ca. 390 °C. Moreover, the FTIR analysis (Figure 6) shows some amount of carbonate ions in the structure of the samples (wide bands around 1370–1460  $\text{cm}^{-1}$ ). This could indicate hydrotalcite as one of the components of the samples. According to [10,24], the emission of carbon dioxide in hydrotalcite takes place in the range of 400–580 °C and the loss of mass connected with that is small and stretched over a long range of temperatures. However, taking all the facts into consideration, it can be stated that the hydrated double phase present in the samples is a mixture of double magnesium aluminum hydroxide hydrate with a poorly crystalline hydrotalcite-like phase. This would explain lack of this phase on the XRD spectra. Based on this, it can be stated that the studied samples are composed of aluminum oxide, aluminum oxide hydrate, boehmite, brucite, and a mixture of poorly crystalline hydrotalcite-like phase and double magnesium alumina hydroxide hydrate. Moreover, in the samples with an addition of chelates, traces of  $\text{MgO}$  are also present.

According to the thermal analysis (Figure 4), FTIR analysis (Figure 6) as well as the XRD analysis results (Figure 5d), the influence of the chelates on the amount of the mixture of hydrotalcite-like phase and double magnesium alumina hydroxide hydrate can be observed. With the addition of acids, the amount of this mixture increases by around 1% (based on the TG curve), which is confirmed by the XRD analysis (Figure 5d), where the intensity of the diffractive lines for the double magnesium and alumina hydroxide hydrate is higher for these samples. Moreover, the FTIR analysis shows a higher relative intensity of the bands from carbonate anion, connected with hydrotalcite-like phase, for the samples with acids additions. Simultaneously, we can observe the XRD spectra traces of  $\text{MgO}$  and also a decrease in the amount of brucite (Figure 5c) for samples 2 and 3. This difference, based on the TG curve, is around 0.6%, but this is connected both with the decomposition of brucite as well as the mixture of hydrotalcite-like phase and double magnesium alumina hydroxide hydrate. These latter compounds decrease the difference in mass loss between the reference sample and the samples with the additives. Taking all these facts into consideration, it can be stated that the addition of acids increases the content of the double hydroxide and hydrotalcite-like phase, and decreases the amount of brucite. These aspects can be connected with a well-known anti-hydration effect of chelate compounds. The mechanism of their action is connected with the adsorption and changing of the surface electric charge of ceramic phases as well as the creation of coordination compounds with metal ions preventing the fast precipitation of hydrated phases. During the hydration of  $\text{MgO}$ , the surface of the grains is protonated by protons from water, after that it creates a complex with  $\text{-OH}$  groups from water which dissolve in water [30]. This increases the pH and is followed by the dissociation of the citric as well as tartaric acid. Citric acid in pH above 8 is fully dissociated to form  $\text{C}_6\text{H}_5\text{O}_7^{3-}$ , similarly, the tartaric acid in a fully dissociated form has the formula  $\text{C}_4\text{H}_4\text{O}_6^{2-}$ . Both of them have high potential to adsorb on the  $\text{MgO}$  grains and decrease their hydration; while in the solution, they coordinate

Mg and Al ions inhibiting their precipitation as hydroxide [14,16]. This last effect probably promotes the synthesis of the layered hydroxide-like hydrotalcite and double magnesium alumina hydroxide hydrate.

This aspect looks similar in the case of alumina, the samples with the addition of chelates have a lower content of boehmite (according to the thermal analysis by around 1.4 and 1.7% for samples 2 and 3, respectively) but higher in aluminum oxide (Figure 5a). This could also be connected with the transformations of aluminum hydroxide and/or aluminum oxide. Based on the conducted analysis, in the studied samples there was no evidence of alumina hydroxide compound, although it was an expected intermediate phase, during the increase in the temperature to the maximum value (240 °C) assumed in the experiment. According to the different authors, gibbsite transforms to boehmite in temperatures from 130 °C [20], 150 [19] or 220–230 °C while to bayerite these were at around 280–300 °C [22]. Moreover, some authors state that under temperature exceeding 130–150 °C, boehmite can be directly created from the alumina as a stable phase [18–21]. Based on that, it can be concluded that the absence of the aluminum hydroxide is connected with its fast decomposition to boehmite during the experiment (during the increase in temperature up to the assumed 240 °C), but this conclusion needs further investigation.

Nevertheless, this work proves that the presence of chelate compound modified the behavior of the castables during the heat treatment. This is connected with the changes of the content of the hydraulic phases, the increase in the content of hydrotalcite and double magnesium and aluminum hydroxide hydrate, with a simultaneous decrease in brucite and boehmite content. These facts can be used in the better matching of heat treatment conditions during the preparation of the castables. Moreover, some of these compounds like hydrotalcite and double magnesium and aluminum hydroxide hydrate may decrease the synthesis temperature of the spinel phase [9]. This is probably connected with the thermal decomposition of these compounds with the creation of an amorphous, metastable, mixed oxide solution [24]. By controlling the processes in the studied range of temperatures, we can influence the reactions that occur at a higher temperature and finally the properties of the castables.

## 5. Conclusions

The current work based on the obtained results shows a strong influence of even small amounts of citric and tartaric acids on the hydration of the MgO–Al<sub>2</sub>O<sub>3</sub> system under hydrothermal conditions. Based on this study, several conclusions can be drawn:

- The addition of citric and tartaric acid does not change the phase composition a lot, but change the content of each phase in the samples during the hydrothermal treatment;
- The citric and tartaric acid additives show an anti-hydration effect in relation to MgO;
- The citric and tartaric acid additives decrease the content of boehmite and probably brucite in relation to the reference sample;
- The citric and tartaric acid additives increase the content of mixture double magnesium aluminum hydroxide hydrate and hydrotalcite-like phases in relation to the reference sample;
- There are probably no significant differences between tartaric and citric acid with regard to their influence on the studied samples in the experimental conditions.

The obtained results can be useful for a better understanding of the changes that take place during the heat treatment of refractory castables.

**Author Contributions:** Conceptualization, R.P. and D.M.; methodology, R.P.; software, R.P.; validation, R.P. and D.M.; formal analysis, R.P.; investigation, R.P. and J.R.; resources, D.M.; data curation, D.M., W.N.-W.; writing—original draft preparation, R.P.; writing—review and editing, D.M.; visualization, R.P.; supervision, D.M.; project administration, D.M.; funding acquisition, D.M.; sample preparation, J.R. All authors have read and agreed to the published version of the manuscript.

**Funding:** This study was founded by The National Centre for Research and Development (Poland) within the framework of LIDER VIII project No. LIDER/5/0034/L-8/16/NCBR/2017 (Recipient: D.M.). The sponsor had no role in the design, execution, interpretation, or writing of the study.

**Institutional Review Board Statement:** Not applicable.

**Informed Consent Statement:** Not applicable.

**Data Availability Statement:** Data used in this study are available upon reasonable request to the corresponding author.

**Conflicts of Interest:** The authors declare no conflict of interest.

## References

- Wagner, C. Über den Mechanismus der Bildung von Ionenverbindungen höherer Ordnung (Doppelsalze, Spinelle, Silikate). *Z. Phys. Chem.* **1936**, *34*, 309–316. [\[CrossRef\]](#)
- Li, Y.; Yang, D.; Liu, C.; Yang, P.; Mu, P.; Wen, J.; Chen, S.; Li, Y. Preparation and characterization of novel nonstoichiometric magnesium aluminate spinels. *Ceram. Int.* **2018**, *44*, 15104–15109. [\[CrossRef\]](#)
- Henkel, L.; Koch, D.; Grathwohl, G. MgAl<sub>2</sub>O<sub>4</sub>-Spinel Synthesized by High-Energy Ball Milling and Reaction Sintering. *J. Am. Ceram. Soc.* **2009**, *92*, 805–811. [\[CrossRef\]](#)
- Liu, J.; Lv, X.; Li, J.; Jiang, L. Pressureless sintered magnesium aluminate spinel with enhanced mechanical properties obtained by the two-step sintering method. *J. Alloys Compd.* **2016**, *680*, 133–138. [\[CrossRef\]](#)
- Ganesh, I.; Bhattacharjee, S.; Saha, B.; Johnson, R.; Mahajan, Y. A new sintering aid for magnesium aluminate spinel. *Ceram. Int.* **2001**, *27*, 773–779. [\[CrossRef\]](#)
- Mohan, S.K.; Sarkar, R. A comparative study on the effect of different additives on the formation and densification of magnesium aluminate spinel. *Ceram. Int.* **2016**, *42*, 13932–13943. [\[CrossRef\]](#)
- Sarkar, R.; Das, S.; Banerjee, G. Effect of additives on the densification of reaction sintered and presynthesized spinels. *Ceram. Int.* **2003**, *29*, 55–59. [\[CrossRef\]](#)
- Kim, T.; Kim, N.; Kang, S. Effect of additives on the sintering of MgAl<sub>2</sub>O<sub>4</sub>. *J. Alloy. Compd.* **2014**, *587*, 594–599. [\[CrossRef\]](#)
- Madej, D.; Tyrała, K. In Situ Spinel Formation in a Smart Nano-Structured Matrix for No-Cement Refractory Castables. *Materials* **2020**, *13*, 1403. [\[CrossRef\]](#)
- Prorok, R.; Madej, D. Influence of hydrothermal conditions on the phase composition of materials from the system MgO-Al<sub>2</sub>O<sub>3</sub>-SiO<sub>2</sub>-H<sub>2</sub>O. *J. Aust. Ceram. Soc.* **2020**, *56*, 829–837. [\[CrossRef\]](#)
- Madej, D.; Prorok, R.; Wiśniewska, K. An experimental investigation of hydration mechanism of the binary cementitious pastes containing MgO and Al<sub>2</sub>O<sub>3</sub> micro-powders. *J. Therm. Anal. Calorim.* **2018**, *134*, 1481–1492. [\[CrossRef\]](#)
- Perander, L.M.; Metson, J.B.; Klett, C. Two Perspectives on the evolution and future of alumina. In *Light Metals*; Lindsay, S.J., Ed.; Springer: Berlin/Heidelberg, Germany, 2011.
- Ye, G.; Troczynski, T. Hydration of hydratable alumina in the presence of various forms of MgO. *Ceram. Int.* **2006**, *32*, 257–262. [\[CrossRef\]](#)
- Salomão, R.; Pandolfelli, V. Citric acid as anti-hydration additive for magnesia containing refractory castables. *Ceram. Int.* **2011**, *37*, 1839–1842. [\[CrossRef\]](#)
- Bucur, A.I.; Bucur, R.A.; Szabadai, Z.; Mosoarca, C.; Linul, P.A. Influence of small concentration addition of tartaric acid on the 220 °C hydrothermal synthesis of hydroxyapatite. *Mater. Charact.* **2017**, *132*, 76–82. [\[CrossRef\]](#)
- Martínez, A.; Vargas, R.; Galano, A. Citric acid: A promising copper scavenger. *Comput. Theor. Chem.* **2018**, *1133*, 47–50. [\[CrossRef\]](#)
- He, Y.; Ye, G.; Troczynski, T.; Oprea, G. Hydration behaviour of magnesia in binder systems for basic castables. *Can. Metall. Q.* **2004**, *43*, 173–176. [\[CrossRef\]](#)
- Serena, S.; Raso, M.; Rodriguez, M.; Caballero, A.; Leo, T. Thermodynamic evaluation of the Al<sub>2</sub>O<sub>3</sub>-H<sub>2</sub>O binary system at pressures up to 30 MPa. *Ceram. Int.* **2009**, *35*, 3081–3090. [\[CrossRef\]](#)
- Laubengayer, A.W.; Weisz, R.S. A hydrothermal study in the system alumina-water. *Am. Chem. Soc. J.* **1943**, *65*, 247–250. [\[CrossRef\]](#)
- Ervin, G.; Osborn, E.F. The system Al<sub>2</sub>O<sub>3</sub>-H<sub>2</sub>O. *J. Geol.* **1951**, *59*, 381–394.
- Al'Myasheva, O.V.; Korytkova, E.N.; Maslov, A.V.; Gusarov, V.V. Preparation of Nanocrystalline Alumina under Hydrothermal Conditions. *Inorg. Mater.* **2005**, *41*, 460–467. [\[CrossRef\]](#)
- Collier, N.C. Transition and decomposition temperatures of cement phases—A collection of thermal analysis data. *Ceram. Silik.* **2016**, *60*, 338–343. [\[CrossRef\]](#)
- Madej, D. Size-dependent hydration mechanism and kinetics for reactive MgO and Al<sub>2</sub>O<sub>3</sub> powders with respect to the calcia-free hydraulic binder systems designed for refractory castables. *J. Mater. Sci.* **2017**, *41*, 176–7590. [\[CrossRef\]](#)
- Yang, W.; Kim, Y.; Liu, P.K.; Sahimi, M.; Tsotsis, T.T. A study by in situ techniques of the thermal evolution of the structure of a Mg-Al-CO<sub>3</sub> layered double hydroxide. *Chem. Eng. Sci.* **2002**, *57*, 2945–2953. [\[CrossRef\]](#)
- Hollingbery, L.; Hull, T. The thermal decomposition of huntite and hydromagnesite—A review. *Thermochim. Acta* **2010**, *509*, 1–11. [\[CrossRef\]](#)

- 
26. Frost, R.L.; Kloprogge, J. Infrared emission spectroscopic study of brucite. *Spectrochim. Acta Part A Mol. Biomol. Spectrosc.* **1999**, *55*, 2195–2205. [[CrossRef](#)]
  27. Frost, R.L.; Locos, B.O.; Ruan, H.; Kloprogge, J.T. Near-infrared and mid infrared spectroscopic study sepiolites and palygorskites. *Vib. Spectrosc.* **2001**, *27*, 1–13. [[CrossRef](#)]
  28. Liu, C.; Shih, K.; Gao, Y.; Li, F.; Wei, L. Dechlorinating transformation of propachlor through nucleophilic substitution by dithionite on the surface of alumina. *J. Soils Sediments* **2012**, *12*, 724–733. [[CrossRef](#)]
  29. Kloprogge, J.; Frost, R.L. Fourier Transform Infrared and Raman Spectroscopic Study of the Local Structure of Mg-, Ni-, and Co-Hydrotalcites. *J. Solid State Chem.* **1999**, *146*, 506–515. [[CrossRef](#)]
  30. Vermilyea, D.A. The Dissolution of MgO and Mg(OH)<sub>2</sub> in Aqueous Solutions. *J. Electrochem. Soc.* **1969**, *116*, 1179–1183. [[CrossRef](#)]